**Specialty Journal of Pharmacognosy, Phytochemistry, and Biotechnology**
**ISSN: 3062-441X**
2024, Volume 4, Page No: 183-199

Available online at: www.galaxypub.co/page/journals

**Galaxy Publication**

# Comprehensive Glycosylation Risk Score Stratifies Bladder Cancer Prognosis and Immunotherapeutic Benefit Across Multi-Cohort and Real-World Data

**Sergei Ivanov[1]*, Dmitry Petrov[1], Alexei Smirnov[1]**

[1]Department of Pharmacognosy, Faculty of Pharmacy, Sechenov University, Moscow, Russia.

***E-mail** ✉ sergei.ivanov.pg@outlook.com

**Received:** 28 May 2024; **Revised:** 06 September 2024; **Accepted:** 11 September 2024

## ABSTRACT

Bladder cancer represents a frequently encountered urologic malignancy and is linked to considerable morbidity and mortality. Although immunotherapy has become an important therapeutic approach, patient responses vary widely. Altered glycosylation has been associated with cancer development and immune modulation. Nevertheless, an integrated view of how glycosylation contributes to bladder cancer progression and its clinical relevance remains insufficiently defined. A training cohort was generated using the TCGA-BLCA dataset. Additional datasets from Xiangya Hospital and public repositories (Xiangya cohort, GSE32894, GSE48075, GSE31684, GSE69795, and E-MTAB-1803) served as validation cohorts. To screen for glycosylation-associated genes linked to prognosis, we applied univariate Cox analysis followed by LASSO regression. A Cox proportional hazards model was then used to construct a risk-scoring system. Kaplan–Meier and ROC analyses evaluated the predictive performance of this score within the training set, and the model was subsequently examined across multiple external datasets.

Based on glycosylation-related gene expression, the training cohort patients were divided into two molecular categories, Cluster 1 and Cluster 2. Survival assessments showed that Cluster 2 had significantly worse outcomes. This cluster also displayed elevated immune-cell infiltration within the tumor microenvironment and stronger activation of major steps in the cancer-immunity cycle. We created an independent prognostic signature ($p < 0.001$) and incorporated it into a nomogram with robust predictive ability. Individuals with a high glycosylation-related risk score demonstrated increased immune infiltration, higher enrichment in immune-therapy-associated pathways, and a pattern consistent with a basal molecular phenotype. In contrast, the low-risk group showed sparse immune-cell infiltration and a luminal-type profile. These patterns were replicated in the real-world Xiangya cohort. This multi-omics glycosylation-based scoring system effectively captured tumor heterogeneity in bladder cancer, forecasted immunotherapy responsiveness and molecular subtype, and may support more precise therapeutic decision-making.

**Keywords:** Glycosylation, Multi-omics, Tumor heterogeneity, Immunotherapy response, Molecular subtype, Bladder carcinoma

**How to Cite This Article:** Ivanov S, Petrov D, Smirnov A. Comprehensive Glycosylation Risk Score Stratifies Bladder Cancer Prognosis and Immunotherapeutic Benefit Across Multi-Cohort and Real-World Data. Spec J Pharmacogn Phytochem Biotechnol. 2024;4:183-99. https://doi.org/10.51847/rEjL0Zopl1

## Introduction

Bladder cancer (BLCA) is a globally prevalent malignancy characterized by substantial morbidity and mortality [1]. Approximately three-quarters of patients present with non-muscle-invasive disease (NMIBC), while the rest are diagnosed with either muscle-invasive bladder cancer (MIBC) or metastatic BLCA [2]. Despite the availability of surgery, chemotherapy, and other treatments, individuals with advanced disease often experience poor survival outcomes [3, 4]. Antibodies directed against PD-1 or its ligands have shown encouraging therapeutic activity for metastatic BLCA [5–8]. Nevertheless, only a fraction of patients derive meaningful benefit [9, 10]. Although PD-L1 expression on tumor or immune cells is used to guide PD-1/PD-L1-targeted therapy, it correlates only partially

with treatment efficacy [11]. Therefore, identifying additional biomarkers capable of improving treatment selection remains an urgent need.

The tumor immune microenvironment (TIME) comprises diverse immune cells and immunologically active molecules [12], and its role in immunotherapy has become increasingly emphasized. Chen and Mellman categorized TIME into "immune-inflamed," "immune-excluded," and "immune-desert," each associated with variable sensitivity to immunotherapies [13]. Likewise, Duan *et al*. differentiated tumors into "hot" and "cold" according to immune infiltration levels [14]. Tumors with minimal immune-cell presence—cold or immune-desert types—are typically resistant to immunotherapy [15]. Therapeutic approaches aiming to convert poorly infiltrated tumors into immune-rich "hot" phenotypes are currently being explored [16, 17]. As such, detailed characterization of the TIME is fundamental for improving the effectiveness of immunotherapeutic strategies.

Glycosylation is a widespread post-translational modification found across all life forms [18]. It entails attaching mono- or polysaccharide structures—such as oligosaccharides or more complex glycans—to designated amino acid residues on proteins [19]. This biochemical alteration is known to influence a broad spectrum of cellular activities, including secretion, degradation pathways, intracellular transport, receptor–ligand interactions, and the regulation of immune activity [20, 21]. Aberrant glycosylation patterns have been linked to the development of many common diseases, cancer being a prominent example [19]. Changes in glycan modifications can modulate tumor initiation and progression by affecting cell proliferation, differentiation, metastatic potential, and immune escape. Numerous malignancies, including BLCA, exhibit disrupted glycosylation signatures [22, 23]. For instance, N-glycosylation of cadherin has been associated with the invasive behavior of BLCA cells [22]. Moreover, glycan alterations also play a role in shaping immune dynamics within the tumor immune microenvironment (TIME) [24, 25]. Despite these insights, a detailed characterization of glycosylation patterns in BLCA and their clinical implications remains incomplete. Given its dual involvement in oncogenesis and immune regulation, glycosylation signatures may offer promising biomarkers for forecasting immunotherapy outcomes in BLCA.

The aim of this study is to generate a glycosylation-based risk model using a multi-omics strategy to provide a comprehensive and individualized prediction of prognosis, immune phenotypes, and tumor heterogeneity in patients with BLCA. We also seek to evaluate the clinical utility of this risk score to guide therapeutic decision-making—including precision immunotherapy—and ultimately improve patient outcomes.

## Materials and Methods

### *Data collection*

#### *Training set*

We assembled a cohort of 408 BLCA patients from The Cancer Genome Atlas (TCGA). Their mRNA expression profiles and clinical data were obtained from the Genomic Data Commons (GDC, https://portal.gdc.cancer.gov/) [26]. The fragments per kilobase of exon per million mapped reads (FPKM) and raw counts in the original dataset were converted to transcripts per kilobase per million (TPM). After integrating these values with clinical annotations, we removed 5 cases due to duplicated entries or missing follow-up information, leaving 403 patients for the training cohort.

#### *Validation cohorts*

In our previous work [27], we developed the Xiangya cohort, which has been deposited in the GEO database (GSE188715). This set includes 56 BLCA patients with complete survival data and RNA-seq profiles. Additionally, we retrieved four more external validation datasets from GEO (GSE32894, GSE48075, GSE31684, and GSE69795). After excluding duplicate cases and samples lacking survival information, the final numbers included were 224 (GSE32894), 73 (GSE48075), 93 (GSE31684), and 38 (GSE69795). Another dataset, E-MTAB-1803, was downloaded from the ArrayExpress repository (https://www.ebi.ac.uk/arrayexpress/) to provide an additional external validation cohort.

### *Consensus clustering*

We obtained a list of 628 glycosylation-associated genes from gene set enrichment analysis (GSEA). To evaluate their expression patterns within the training dataset, we applied consensus clustering using the "ConsuClusterPlus" R package [28]. The following settings were used: distance = "manhattan", clusterAlg =

"pam", maxK = 5, Reps = 1,500, pItem = 0.8, and pFeature = 1. This approach allowed us to identify distinct glycosylation-related expression subgroups.

*Describing the TIME of BLCA*

To profile the tumor immune microenvironment (TIME) in BLCA, we drew on the tracking tumor immunophenotype (TIP) platform (http://biocc.hrbmu.edu.cn/TIP/) [29], which provided activity scores across the 7 phases of the Cancer Immunity Cycle (CIC) [30]. In addition, we assembled a curated list comprising 22 immune checkpoint inhibitor (ICI)–related genes, 18 markers from the T cell–associated inflammatory signature (TIS), and representative effector genes for $CD8^+$ T cells, dendritic cells (DCs), macrophages, natural killer (NK) cells, and Th1 cells, following criteria from our earlier work [31].

*Development of the glycosylation risk score*

To screen genes linked to glycosylation patterns and patient outcomes, we applied two analytical strategies: univariate Cox regression and the least absolute shrinkage and selection operator (LASSO). The LASSO procedure was executed with the "glmnet" R package. First, univariate Cox testing was run on 628 genes, identifying 30 with strong prognostic relevance ($p < 0.005$). These were next processed by the LASSO algorithm to further narrow the candidates, yielding a set of 20 genes. The final glycosylation-based risk model was then formulated using a Cox proportional hazards framework implemented through "glmnet," incorporating these same 20 genes.

$$\text{GlycosylationScore} = \sum \beta_i \times \text{RNA}_i \quad (1)$$

*Evaluation and verification of the glycosylation risk score*

Within the training cohort, individuals were separated into low- and high-risk categories using the median score as the cutoff. Kaplan–Meier (K-M) curves were generated, and group differences were assessed with the log-rank test using the "survminer" package. Predictive performance was quantified through time-dependent ROC (tROC) analysis via the "tROC" R package. A nomogram combining clinical prognostic variables with the glycosylation score was also built, and its calibration was examined through calibration plots.

For external validation, the same workflow was applied to an independent BLCA dataset. Risk scores were computed using the established equation, and patients were again divided into high- and low-risk strata using the median threshold. Survival distinctions were evaluated with K-M and log-rank tests, and discriminative capacity was examined with tROC curves.

*Identification of molecular subtypes of BLCA using the glycosylation risk score*

In previous research, our group synthesized seven widely used molecular classification systems for BLCA, including schemes from TCGA, UNC, and Consensus-based frameworks. To harmonize subtype assignments, we used the "BLCAsubtyping" and "ConsensusMIBC" R packages. Moreover, pathways and subtype markers reported by Kamoun *et al*. (2020) were incorporated [32]. For improved clinical interpretability, all molecular classes were further consolidated into two overarching groups: "luminal" and "basal."

*Statistical analysis*

Associations among variables were explored using Pearson or Spearman coefficients, chosen according to data distributions. Continuous variables between two groups were compared using either t-tests or Mann–Whitney U tests. Survival was evaluated using the K-M estimator and log-rank significance testing. Candidate prognostic genes were identified by univariate Cox regression, whereas the LASSO procedure refined gene selection for the glycosylation score. Hazard ratios (HRs) and the independent predictive contribution of the glycosylation score were evaluated through univariate and multivariate Cox models. Model performance was measured with time-dependent ROC curves and corresponding area under the curve (AUC) values. All computations were run in R (version 4.22), applying a $p < 0.05$ significance threshold. Multiple-testing correction was conducted using the false discovery rate (FDR), and all statistical tests were two-tailed.

**Results and Discussion**

*Establishing glycosylation-related expression patterns linked to prognosis and the tumor immune microenvironment*

Using the TCGA-BLCA dataset, we applied unsupervised clustering via the "ConsenseClusterPlus" R package to generate expression signatures based on glycosylation-associated genes. The analysis indicated that a two-group solution was optimal, giving rise to glycosylation cluster 1 and glycosylation cluster 2 **(Figure 1a)**. We then compared these two clusters in detail. Regarding survival outcomes, cluster 2 displayed a clearly worse overall prognosis than cluster 1 ($p = 0.024$), **(Figure 1b)**.

For TIME characteristics, as illustrated in **Figure 1c**, most immune infiltrates—including activated and immature B cells, activated and central-memory $CD4^+$ T cells, activated and central-memory $CD8^+$ T cells, NK cells, and macrophages—were present at higher levels in cluster 2. Furthermore, within the seven-step CIC framework, cluster 2 showed more pronounced activation in key anti-cancer immunity phases: step 1 (tumor antigen release), step 4 (recruitment of T cells, $CD8^+$ T cells, macrophages, NK cells, and DCs), step 6 (T-cell recognition of malignant cells), and step 7 (tumor cell elimination) **(Figure 1d)**.

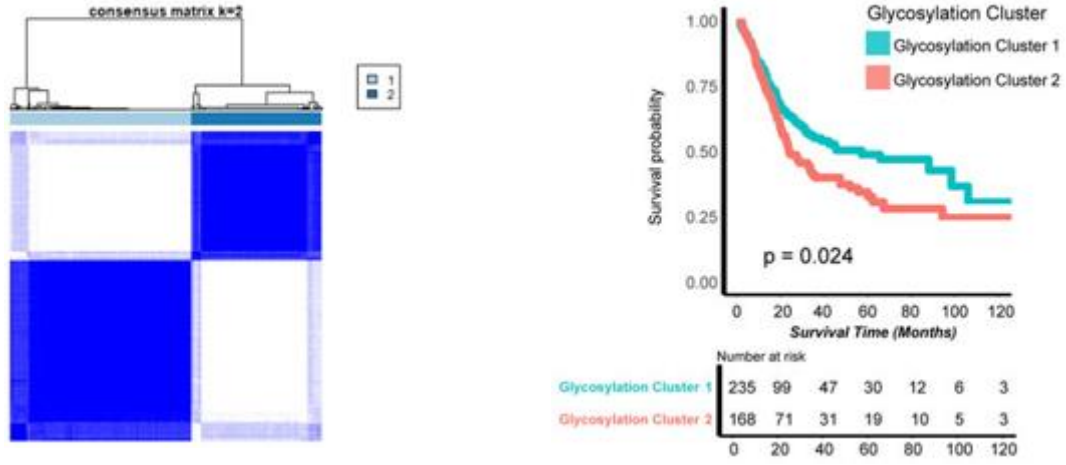


a) b)

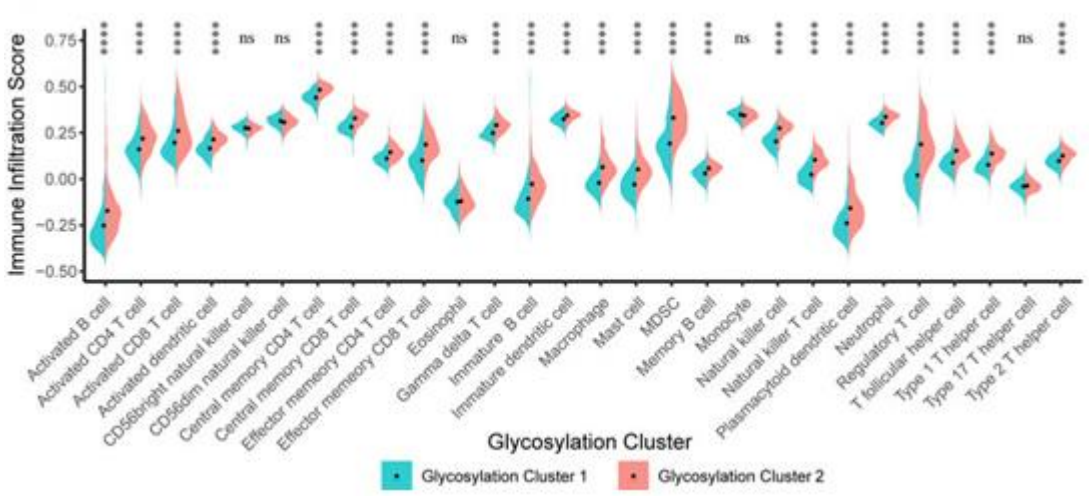


c)

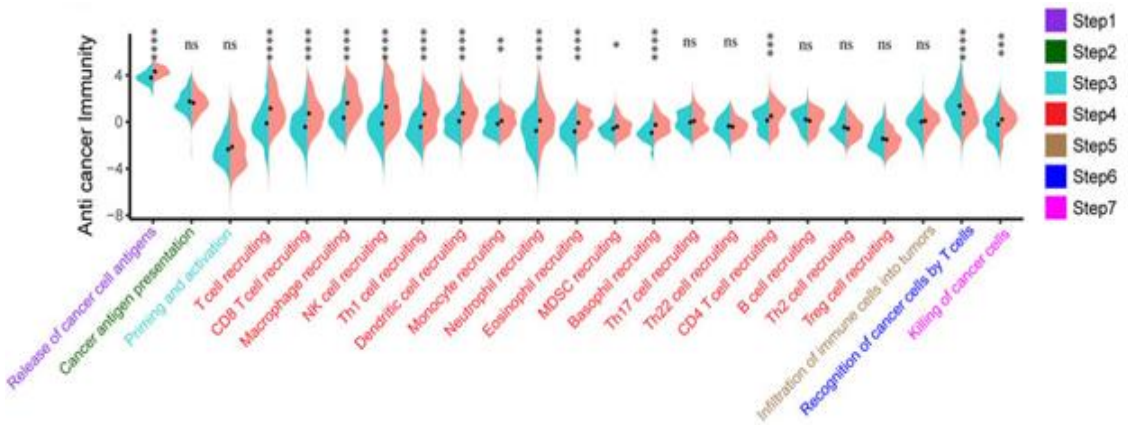


d)

**Figure 1.** Construction of glycosylation-based expression patterns related to clinical outcome and immune contexture.

(a) Unsupervised clustering of all 628 glycosylation-related genes, with light and dark blue denoting clusters 1 and 2.

(b) Kaplan–Meier comparison of OS across the two patterns (light green = cluster 1; red = cluster 2).

(c) Differences in 28 immune-cell infiltration levels using ssGSEA between the two patterns (light green = cluster 1; red = cluster 2). *p < 0.05, **p < 0.01, ***p < 0.001, ****p < 0.0001; ns = non-significant.

(d) Distinct anti-tumor immune activity across CIC steps in the two patterns (light green = cluster 1; red = cluster 2). Same significance indicators as above.

*Developing glycosylation-associated risk scores and evaluating clinical prediction across multiple cohorts*

The marked contrasts between the two glycosylation clusters—both in survival and immune context—motivated us to construct a quantitative scoring system reflecting glycosylation gene behavior. This scoring metric was intended to stratify BLCA patients and support precision-oriented prognosis assessment.

We first performed univariate Cox analysis on glycosylation-related genes and identified 30 genes strongly linked to OS ($p < 0.005$). LASSO regression was then used to reduce this list to 20 optimal prognostic candidates **(Figures 2a and 2b)**. The minimum lambda value, determined through ten-fold cross-validation, was selected as the tuning criterion. Based on these 20 genes, a final Cox proportional hazards model was generated using the "glmnet" package, producing the glycosylation-based risk score for the TCGA-BLCA training cohort. Patients were assigned to high- or low-score groups according to the median risk score.

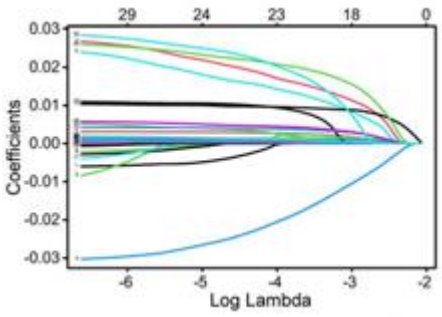


a)

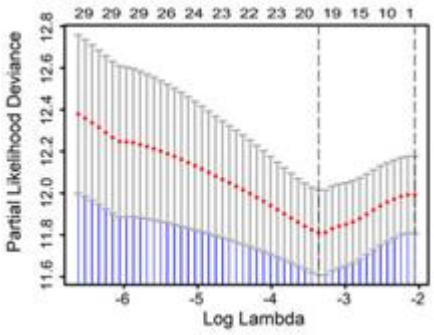


b)

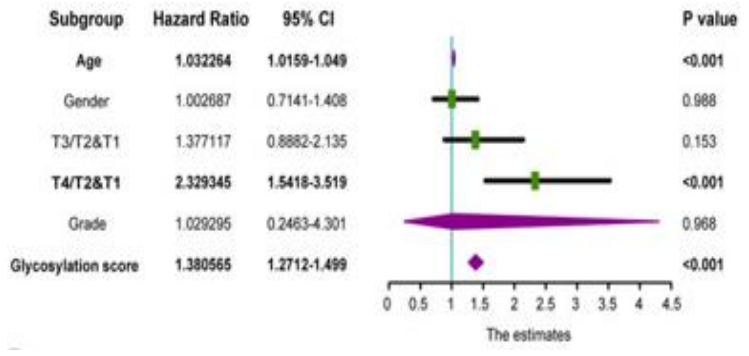


c)

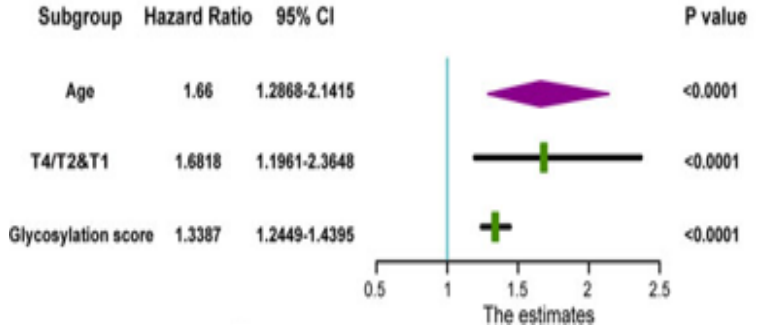


d)

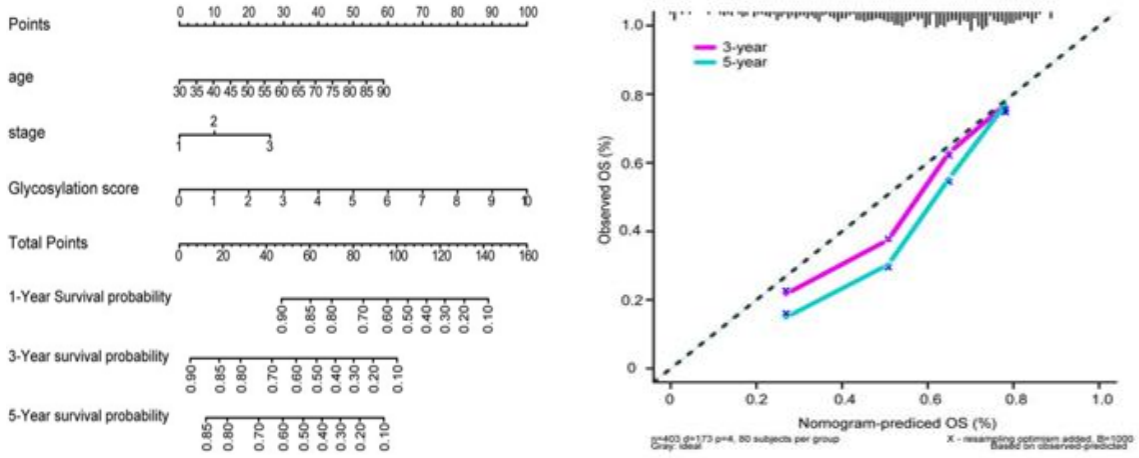


e) f)

**Figure 2.** Development of glycosylation-derived risk score and clinical predictive modeling.
(a) LASSO coefficient profiles of glycosylation-related prognostic genes across lambda values.
(b) Partial likelihood deviance versus log(lambda) with 10-fold cross-validation.
(c–d) Forest plots for univariate and multivariate Cox analyses incorporating age, sex, tumor grade, tumor stage, and the glycosylation-based score.
(e) Nomogram including age, stage, and glycosylation-based risk score.
(f) Calibration curves for nomogram accuracy.

To determine the clinical applicability of the risk score, we first conducted a univariate Cox evaluation. The analysis showed that the glycosylation score—and clinical parameters such as grade, stage, age, and sex—were all significantly prognostic ($p < 0.001$), **(Figure 2c)**. In multivariate Cox analysis, the glycosylation score continued to serve as an independent outcome predictor ($p < 0.001$), **(Figure 2d)**.

Based on factors identified through multivariate modeling (risk score, age, and tumor stage), we generated a glycosylation-focused nomogram **(Figure 2e)**. The score contributed substantially to total prognostic weight, indicating that glycosylation levels are highly informative for predicting 1-, 3-, and 5-year survival. Consistent with earlier findings, higher risk scores corresponded to poorer outcomes, highlighting the clinical need for alternative therapies in these high-risk individuals. Calibration analyses demonstrated that the nomogram's predicted OS closely matched actual observations **(Figure 2f)**, and Q-Q analysis confirmed data normality.

*Validating the prognostic relevance of the glycosylation risk score across multiple BLCA cohorts*

To more comprehensively assess how well the glycosylation risk score predicts outcomes in BLCA, we verified its performance in several datasets, including public cohorts and our own clinical population. In the TCGA-BLCA training set, individuals with elevated glycosylation scores demonstrated a markedly poorer overall survival compared with those in the low-score category ($p < 0.0001$), **(Figure 3a)**. The score also showed strong predictive capability for survival at 1, 3, and 5 years, yielding AUC values of 0.75, 0.74, and 0.75, respectively **(Figure 3b)**. In our real-world Xiangya BLCA cohort, the unfavorable prognosis associated with high scores remained evident ($p = 0.014$), **(Figure 3c)**, and its predictive accuracy remained substantial (1-, 3-, and 5-year AUCs: 0.75, 0.71, and 0.56; **(Figure 3d)**). Comparable findings were consistently observed in several external validation datasets: E-MTAB-1803 ($p = 0.00019$, AUCs: 0.73, 0.76, 0.77); **(Figures 3e and 3f)**, GSE32894 ($p < 0.0001$, AUCs: 0.83, 0.89, 0.88); **(Figures 3g and 3h)**, GSE48075 ($p = 0.00012$, AUCs: 0.82, 0.78, 0.76); **(Figures 3i and 3j)**, and two additional GEO BLCA sets.

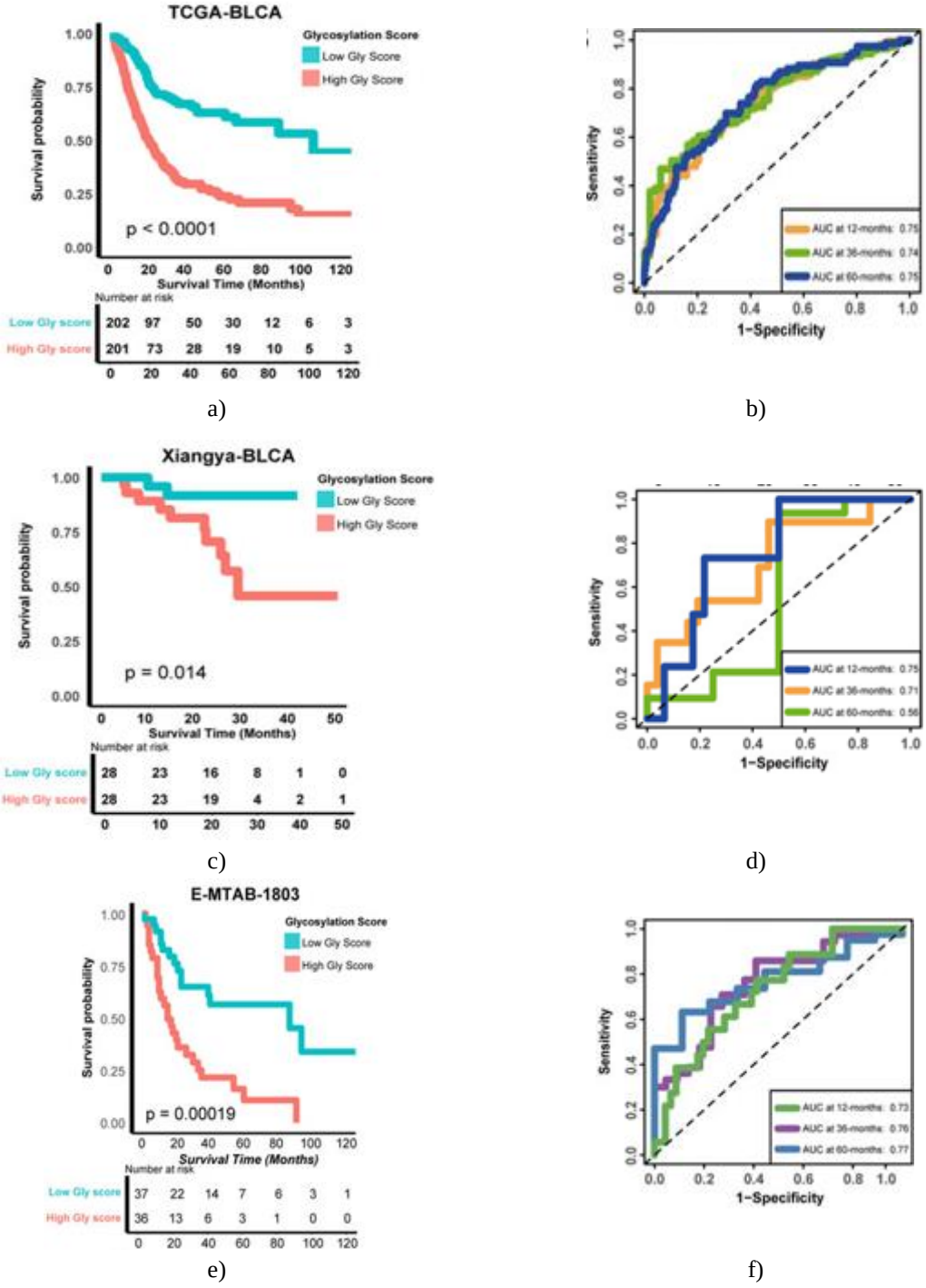

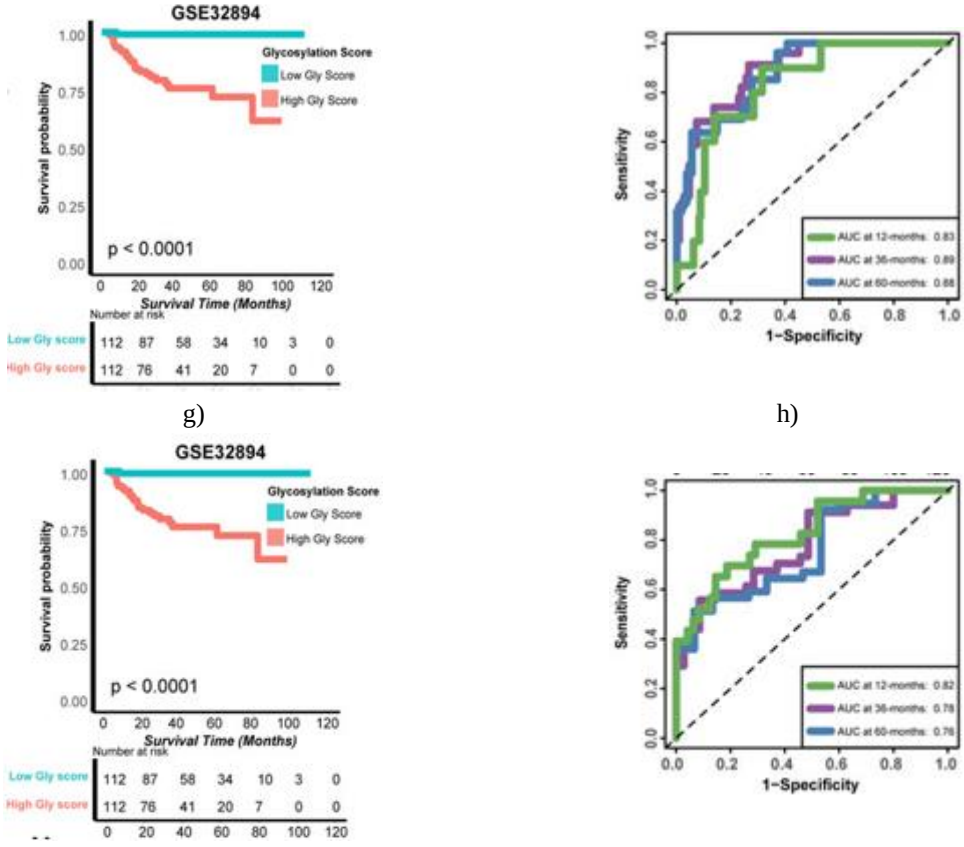


**Figure 3.** Verification of glycosylation risk score in predicting clinical outcome across multiple datasets.
(a) K–M curves for TCGA-BLCA high vs. low score groups (red = high; green = low).
(b) ROC analysis of the score in TCGA-BLCA.
(c–d) K–M curves and ROC plots in the Xiangya validation cohort.
(e–f) K–M and ROC plots in E-MTAB-1803.
(g–h) K–M and ROC plots in GSE32894.
(i–j) K–M and ROC plots in GSE48075.

Collectively, these assessments strongly support that the glycosylation risk score is a stable and accurate prognostic indicator in BLCA, with reliable performance both internally and across external datasets.

*Investigating associations between glycosylation score and the tumor immune microenvironment in TCGA-BLCA*
The compelling prognostic capability of the glycosylation score motivated further analysis of its relationship with the TIME in the TCGA-BLCA cohort. Based on ssGSEA profiling **(Figure 4a)**, immune infiltration was broadly higher in the high-score group, particularly for central-memory $CD8^+/CD4^+$ T cells, NK T cells, NK cells, regulatory T cells, and memory B cells. Correlations between glycosylation score and key immune-cell subsets are illustrated in **Figure 4b**.
Moreover, major components of the 7-step CIC—such as antigen release, immune-cell recruitment, and tumor-cell elimination—were more activated in the high-score group **(Figure 4c)**. We further assessed whether the glycosylation score aligned with the enrichment of 21 immunotherapy-associated pathways summarized by Mariathasan *et al*. (2018) [33]. High-score patients consistently presented elevated enrichment scores across these pathways **(Figure 4d)**.
Finally, drawing upon the TIS metric previously established by our group, we found that individuals with higher glycosylation scores also had elevated TIS values **(Figure 4e)**. Together, these findings indicate that the high glycosylation score subgroup tends to exhibit a “hot” immune phenotype and may be more responsive to immunotherapy.

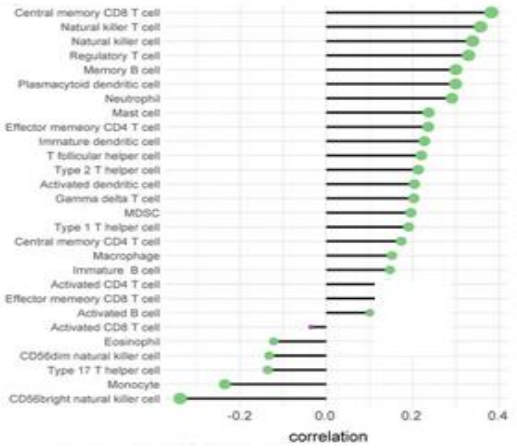


a)

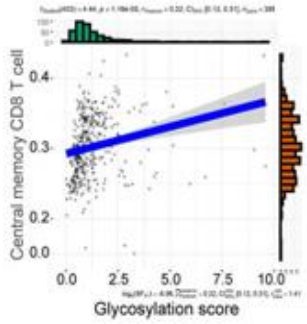


b)

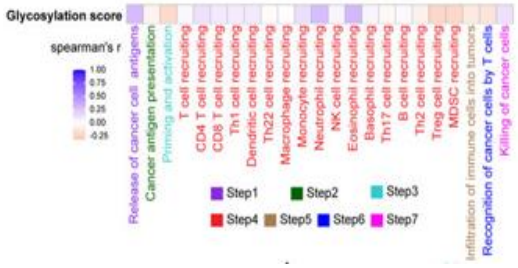


a)

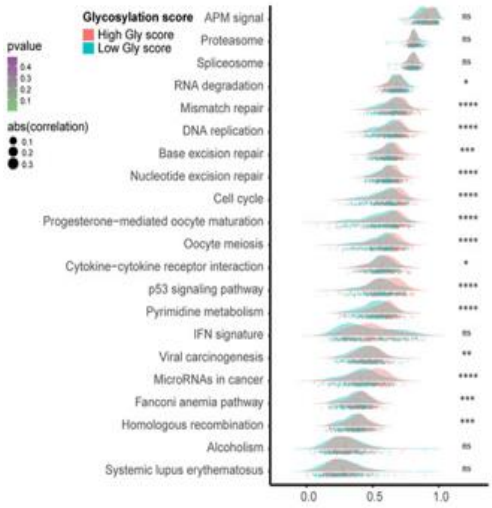


c)

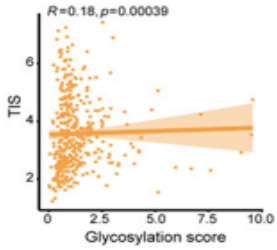


e)

**Figure 4.** Examination of the link between the Glycosylation score and the TIME in the TCGA-BLCA dataset.

(a) Comparison of immune-cell enrichment between high- and low-glycosylation groups in TCGA-BLCA.

(b) Association between central-memory CD8⁺ T-cell abundance and the glycosylation score.

(c) Relationship between the glycosylation score and the activities of cancer-immunity-cycle steps.

(d) Distinct activation levels of ICB-related gene signatures across the two score groups (red = high; green = low; *p < 0.05, **p < 0.01, ***p < 0.001, ****p < 0.0001; ns = not significant).

(e) Correlation between the glycosylation score and the T-cell–inflamed signature (TIS).

*Validation of the glycosylation score–TIME relationship in a real-world BLCA population*

After establishing in TCGA-BLCA that glycosylation levels can infer the immune phenotype of the TME, we next examined this pattern in patients treated at Xiangya Hospital. Consistent with prior observations, key steps of the 7-stage CIC **(Figure 5a),** (left) were more strongly activated among individuals with elevated scores. Parallel to this, immune infiltration within the TME showed a clear increase in the high-score group **(Figure 5a),** (right).

Moreover, as illustrated in **Figure 5b**, individuals with higher scores expressed more ICI-related genes (upper panel) and more TIS-related genes (lower panel), reinforcing the notion of enhanced immune activity. Evaluation of immune-effector signatures further revealed that patients in the high-score category displayed elevated expression of genes characteristic of $CD8^+$ T cells, dendritic cells, macrophages, NK cells, and Th1 cells **(Figure 5c)**.

Integrating evidence from both TCGA-BLCA and Xiangya-BLCA, we conclude that patients with increased glycosylation scores frequently present a “hot” immune microenvironment and therefore may respond more favorably to immunotherapy.

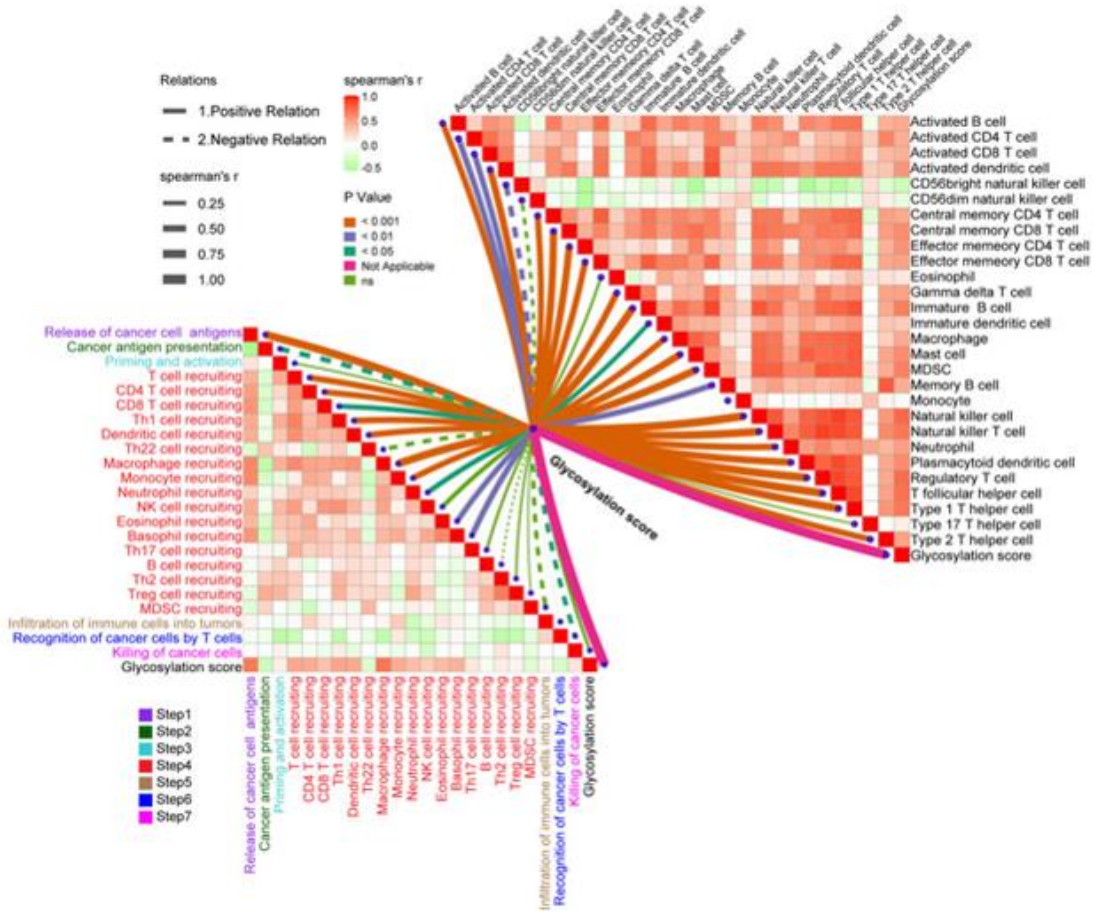


a)

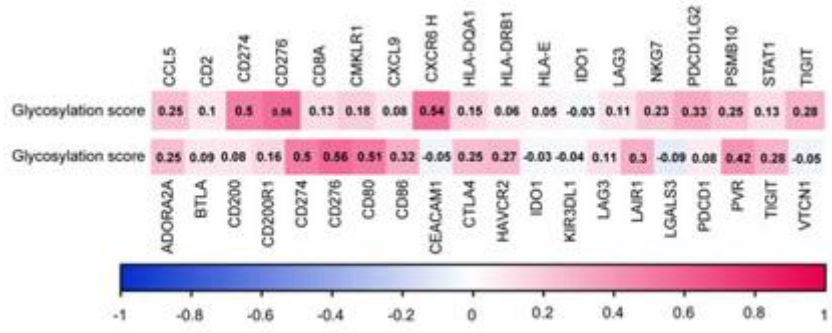


b)

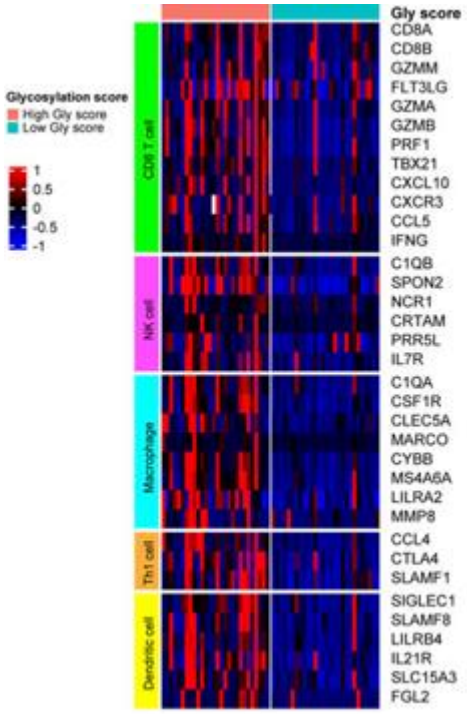


c)

**Figure 5.** Verification of associations between glycosylation score and TIME in real-world BLCA.
(a) Links between glycosylation score and CIC activity (left) and immune-cell infiltration patterns (right). Line type, color, and thickness reflect relation polarity, p-value, and strength, respectively.
(b) Relationship between the glycosylation score and TIS-related genes (upper) and ICI-related genes (lower).
(c) Differences in immune-effector-gene expression between high- and low-score groups (red = high; green = low).

*Glycosylation score as a tool for precision-medicine guidance through prediction of BLCA molecular subtypes*

Expression-based stratification has demonstrated that MIBC comprises diverse biological subgroups with distinct clinical outcomes and treatment sensitivities [34–36]. Widely accepted subtype systems include the consensus [32], TCGA [37], CIT [38], Lund [39], Baylor [40], UNC [41], and MDA [42] classifications. Our earlier work harmonized these seven schemes to streamline clinical use [27].

A notable degree of agreement was observed between the TCGA-BLCA dataset **(Figure 6a)**, (top) and our Xiangya cohort **(Figure 6a)**, (bottom). Across classification systems, basal-type tumors generally displayed higher glycosylation scores, whereas luminal-type tumors tended to have lower scores. High-score patients preferentially demonstrated basal-type traits, including EMT-related, immune-related, basal-related, and interferon-related differentiation. Conversely, low-score individuals more often fitted luminal or urothelial differentiation patterns.

Regarding subtype-prediction accuracy, in TCGA-BLCA **(Figure 6b)**, most AUC values exceeded 0.73, while in the Xiangya cohort **(Figure 6c)**, most surpassed 0.87.

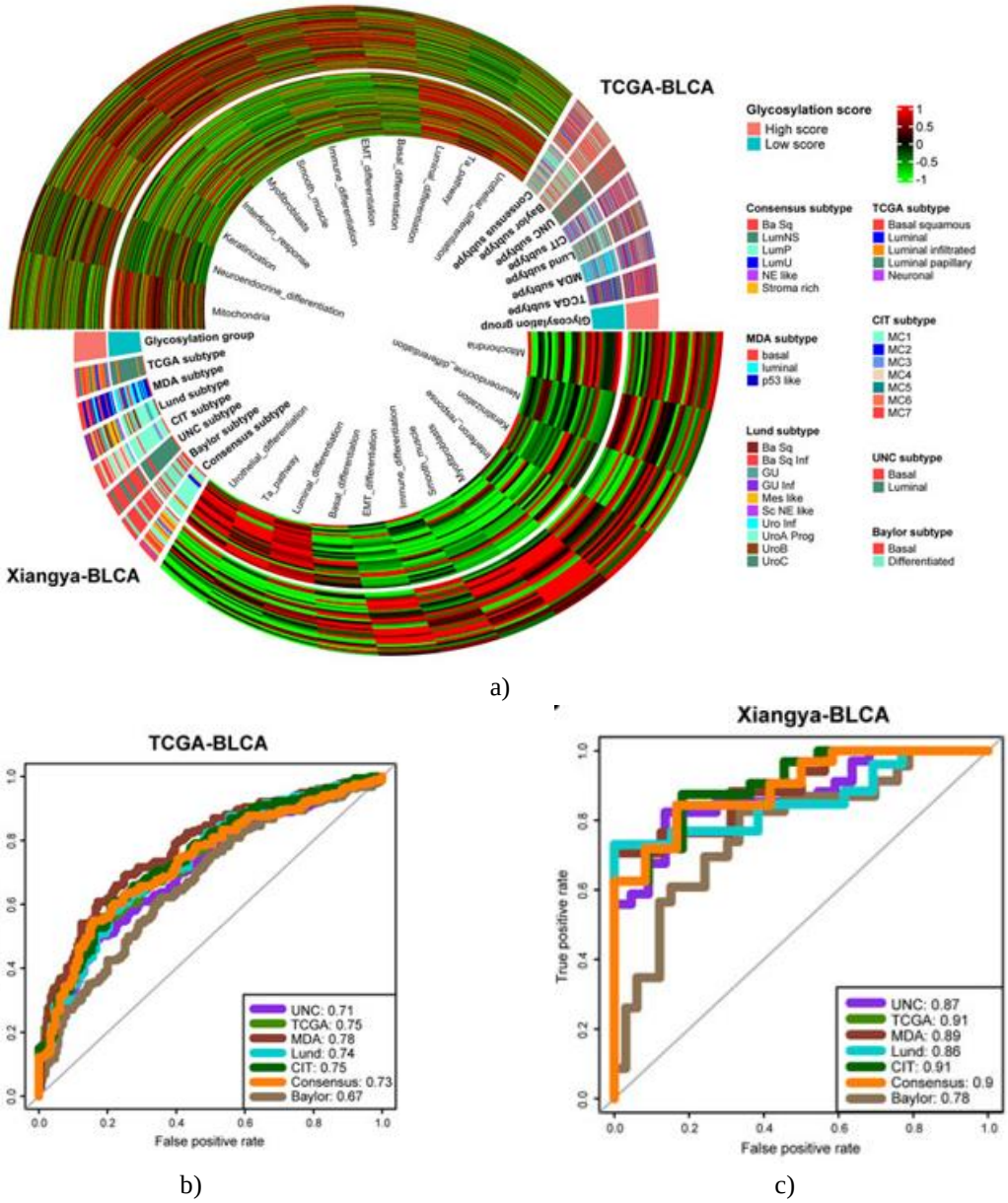


a)




b) c)

**Figure 6.** Glycosylation score–based guidance of precision-therapy by predicting BLCA molecular subtypes (a) Heatmaps showing glycosylation-score groups, seven subtype systems, and BLCA-related signatures in TCGA-BLCA (top) and Xiangya (bottom). Activated pathways appear in red; suppressed pathways in green. (b–c) ROC performance of the glycosylation score for predicting subtype classifications in TCGA-BLCA and Xiangya cohorts.

Earlier analyses [32, 43] reported that basal-type BLCA typically exhibits lower differentiation and thus worse prognosis, but responds more strongly to therapies such as cisplatin and ICB. In line with this, our work demonstrates that patients with elevated glycosylation scores—who more often show basal-like features—have poorer survival yet higher immune infiltration, aligning with enhanced sensitivity to immunotherapy.

Cisplatin-based neoadjuvant chemotherapy, followed by radical cystectomy and urinary diversion, has remained the mainstream therapeutic strategy for locally advanced MIBC since the early 2000s [44, 45]. Protein glycosylation—one of the most prevalent post-translational modifications—participates in essential biological processes such as cellular motility, intercellular communication, proliferation, and adhesion [46]. Dysregulated glycosylation is also recognized as a critical contributor to tumor initiation and progression [47], including in BLCA. Investigations into protein modification, tumor heterogeneity, and predictors of immunotherapeutic responsiveness (e.g., ICB) continue to attract considerable interest across malignancies [48, 49]. Accordingly, our study aimed to thoroughly examine the interplay between glycosylation pathways and BLCA, with the intent of improving prognostic assessment and optimizing individualized therapeutic strategies.

To begin with, using the expression profiles of 628 glycosylation-related genes in TCGA-BLCA cases, we employed consensus clustering to define two optimal groups, termed glycosylation cluster 1 and glycosylation cluster 2. Patients in glycosylation cluster 2 exhibited inferior survival while showing increased immune infiltration within the TME. Poor clinical outcomes and suboptimal treatment responses are closely tied to the intricate nature of the TME [50], where immune components and associated pathways play pivotal roles. This motivated us to quantify the prognostic and immunologic significance of glycosylation in BLCA. Although recent mechanistic studies have advanced our understanding of glycosylation in BLCA [51, 52], tools for evaluating prognosis based on glycosylation profiles remain insufficient. Therefore, we developed a scoring model by selecting prognostically relevant genes that best represented glycosylation-associated expression patterns, resulting in the first glycosylation risk score capable of simultaneously predicting survival, immune phenotypes, and molecular subtypes of BLCA.

Cancer cells typically exhibit accelerated protein glycosylation relative to normal tissues [53], and a prospective multi-omics ovarian cancer study by Hu *et al*. (2020) [54] further demonstrated marked differences in glycosylation intensity between malignant and normal cells, which could be captured through glycoprotein expression. Additional evidence has shown that aberrant alterations in glycosylation genes, such as GALNT1, promote tumor development across several cancer types, including BLCA [55]. Moreover, the functional status of tumor-infiltrating immune cells (TIICs), particularly tumor-infiltrating lymphocytes (TILs), is a decisive determinant of patient outcomes [56], including in early-stage pT1 BLCA [57]. New molecular targets—such as BCAT2, EMT-associated signatures, and S100A5 [58–60]—are increasingly shaping immunotherapeutic strategies for BLCA. Evidence from a multicenter cohort of 709 individuals [61] indicated that high-risk BLCA patients following surgery benefit from adjuvant nivolumab. In our analysis, high glycosylation scores were associated with poorer survival but were simultaneously linked to a “hot” TIME [14] characterized by abundant immune infiltration. This trend was consistently observed in both the TCGA-BLCA training cohort and the Xiangya-BLCA real-world dataset. Supporting this, Badmann *et al*. (2020) proposed that in ovarian cancer [24], enhanced glycosylation may drive macrophages toward an anti-inflammatory M2 phenotype, thereby fostering immune escape even within an otherwise activated TME.

Previous investigations have demonstrated that molecular classification systems can enhance the precision of prognostic evaluation and the characterization of the tumor immune microenvironment. In breast cancer research, for instance, notable disparities in TIL infiltration levels were observed across HR+ molecular categories, where increased TIL presence improved OS but did not extend disease-free survival (DFS) [62]. In other words, distinct molecular classes correspond to different TIME features [63]. Updating and reconsidering tumor molecular typing frameworks—whether by refining, merging, or simplifying—has therefore become an active research direction. Examples include the 5-mC regulator–based subtype system previously developed by our group, which achieved accurate molecular classification in BLCA [64], as well as a consensus molecular stratification for gastric adenocarcinoma (GAC) aimed at reclassification and predicting ICB response rates [65]. Additionally, our team proposed an integrated system combining several mainstream BLCA molecular subtype standards to better align typing methods with clinical practice [27]. Further supporting the relevance of glycosylation, Miao *et al*. (2022) documented that the glycosylation-associated protein B3GNT5 was markedly upregulated in basal-like breast cancer (BLBR), highlighting a strong link between glycosylation and subtype identity [66]. In the present work, BLCA individuals with elevated glycosylation scores were more likely to fall into basal-type categories and displayed a “hot” TIME, despite experiencing less favorable survival outcomes. Conversely, low glycosylation scores corresponded to luminal-type differentiation, with a matching prognosis and immune profile. Altogether, patients with high glycosylation scores may benefit more from immunotherapies such as ICB, underscoring the need to further expand immunotherapeutic strategies to improve post-treatment outcomes. Meanwhile, patients with low glycosylation scores may require a stronger emphasis on targeted or alternative treatment approaches. These findings further align with earlier studies examining the effect of molecular subtype on tumor prognosis and immune behavior [42, 67].

There are, nevertheless, limitations that warrant further investigation. First, the datasets used were retrospective, meaning the associations among glycosylation, clinical outcome, immune characteristics, and molecular subtype in BLCA primarily remain correlational. Therefore, we aim to adopt this work as a preliminary foundation and conduct prospective studies to evaluate the effects of glycosylation on immunotherapy and targeted therapy in BLCA. Additionally, integrating the current results with an expanded literature review and feasible laboratory approaches, we plan to explore the mechanistic pathways through which glycosylation-related genes influence

BLCA treatment responses, with the goal of identifying new therapeutic targets that can support precision oncology in BLCA.

**Conclusion**

Using multi-omics datasets, we established a glycosylation score associated with BLCA and applied it to predict tumor heterogeneity, clinical outcome, and immune characteristics. The glycosylation score offers reliable prognostic value for immunotherapy response and BLCA molecular subtype assignment, supporting more tailored clinical decision-making for BLCA management.

**Acknowledgments:** None

**Conflict of Interest:** None

**Financial Support:** None

**Ethics Statement:** None

**References**

1. Siegel RL, Miller KD, Jemal A, Fedewa SA, Butterly LF, Anderson JC, et al. Colorectal cancer statistics, 2020. CA Cancer J Clin. 2020;70(1):145–64. doi:10.3322/caac.21601
2. Powles T, Bellmunt J, Comperat E, De Santis M, Huddart R, Loriot Y, et al. Bladder cancer: ESMO clinical practice guideline for diagnosis, treatment and follow-up. Ann Oncol. 2022;33(3):244–58. doi:10.1016/j.annonc.2021.11.012
3. Antoni S, Ferlay J, Soerjomataram I, Znaor A, Jemal A, Bray F. Bladder cancer incidence and mortality: a global overview and recent trends. Eur Urol. 2017;71(1):96–108. doi:10.1016/j.eururo.2016.06.010
4. Lenis AT, Lec PM, Chamie K, Mshs MD. Bladder cancer: A review. JAMA. 2020;324(19):1980–1991. doi:10.1001/jama.2020.17598
5. Rosenberg JE, Hoffman-Censits J, Powles T, van der Heijden MS, Balar AV, Necchi A, et al. Atezolizumab in patients with locally advanced and metastatic urothelial carcinoma who have progressed following treatment with platinum-based chemotherapy: A single-arm, multicentre, phase 2 trial. Lancet. 2016;387(10031):1909–19. doi:10.1016/S0140-6736(16)00561-4
6. Plimack ER, Bellmunt J, Gupta S, Berger R, Chow LQM, Juco J, et al. Safety and activity of pembrolizumab in patients with locally advanced or metastatic urothelial cancer (KEYNOTE-012): A non-randomised, open-label, phase 1b study. Lancet Oncol. 2017;18(2):212–20. doi:10.1016/S1470-2045(17)30007-4
7. Rijnders M, de Wit R, Boormans JL, Lolkema MPJ, van der Veldt AAM. Systematic review of immune checkpoint inhibition in urological cancers. Eur Urol. 2017;72(3):411–23. doi:10.1016/j.eururo.2017.06.012
8. Hu J, Chen J, Ou Z, Chen H, Liu Z, Chen M, et al. Neoadjuvant immunotherapy, chemotherapy, and combination therapy in muscle-invasive bladder cancer: A multicenter real-world retrospective study. Cell Rep Med. 2022;3(11):100785. doi:10.1016/j.xcrm.2022.100785
9. Jenkins RW, Barbie DA, Flaherty KT. Mechanisms of resistance to immune checkpoint inhibitors. Br J Cancer. 2018;118(1):9–16. doi:10.1038/bjc.2017.434
10. Schoenfeld AJ, Hellmann MD. Acquired resistance to immune checkpoint inhibitors. Cancer Cell. 2020;37(4):443–55. doi:10.1016/j.ccell.2020.03.017
11. Ma W, Gilligan BM, Yuan J, Li T. Current status and perspectives in translational biomarker research for PD-1/PD-L1 immune checkpoint blockade therapy. J Hematol Oncol. 2016;9(1):47. doi:10.1186/s13045-016-0277-y
12. Binnewies M, Roberts EW, Kersten K, Chan V, Fearon DF, Merad M, et al. Understanding the tumor immune microenvironment (TIME) for effective therapy. Nat Med. 2018;24(5):541–50. doi:10.1038/s41591-018-0014-x
13. Chen DS, Mellman I. Elements of cancer immunity and the cancer–immune set point. Nature. 2017;541(7637):321–30. doi:10.1038/nature21349

14. Duan Q, Zhang H, Zheng J, Zhang L. Turning cold into hot: firing up the tumor microenvironment. Trends Cancer. 2020;6(7):605–18. doi:10.1016/j.trecan.2020.02.022
15. Galon J, Bruni D. Approaches to treat immune hot, altered and cold tumours with combination immunotherapies. Nat Rev Drug Discov. 2019;18(3):197–218. doi:10.1038/s41573-018-0007-y
16. Bonaventura P, Shekarian T, Alcazer V, Valladeau-Guilemond J, Valsesia-Wittmann S, Amigorena S, et al. Cold tumors: A therapeutic challenge for immunotherapy. Front Immunol. 2019;10(168):168. doi:10.3389/fimmu.2019.00168
17. Vonderheide RH. CD40 agonist antibodies in cancer immunotherapy. Annu Rev Med. 2020;71(1):47–58. doi:10.1146/annurev-med-062518-045435
18. Pinho SS, Reis CA. Glycosylation in cancer: mechanisms and clinical implications. Nat Rev Cancer. 2015;15(9):540–55. doi:10.1038/nrc3982
19. Eichler J. Protein glycosylation. Curr Biol. 2019;29(7):R229–31. doi:10.1016/j.cub.2019.01.003
20. Moremen KW, Tiemeyer M, Nairn AV. Vertebrate protein glycosylation: diversity, synthesis and function. Nat Rev Mol Cell Biol. 2012;13(7):448–62. doi:10.1038/nrm3383
21. Varki A. Biological roles of glycans. Glycobiology. 2017;27(1):3–49. doi:10.1093/glycob/cww086
22. Przybylo M, Hoja-Lukowicz D, Litynska A, Laidler P. Different glycosylation of cadherins from human bladder non-malignant and cancer cell lines. Cancer Cell Int. 2002;2(1):6. doi:10.1186/1475-2867-2-6
23. Rodríguez E, Schetters STT, van Kooyk Y. The tumour glyco-code as a novel immune checkpoint for immunotherapy. Nat Rev Immunol. 2018;18(3):204–11. doi:10.1038/nri.2018.3
24. Badmann S, Heublein S, Mayr D, Reischer A, Liao Y, Kolben T, et al. M2 macrophages infiltrating epithelial ovarian cancer express MDR1: A feature that may account for the poor prognosis. Cells. 2020;9(5):1224. doi:10.3390/cells9051224
25. Sun R, Kim AMJ, Lim SO. Glycosylation of immune receptors in cancer. Cells. 2021;10(5):1100. doi:10.3390/cells10051100
26. Colaprico A, Silva TC, Olsen C, Garofano L, Cava C, Garolini D, et al. TCGAbiolinks: An R/bioconductor package for integrative analysis of TCGA data. Nucleic Acids Res. 2016;44(8):e71. doi:10.1093/nar/gkv1507
27. Li H, Liu S, Li C, Xiao Z, Hu J, Zhao C. TNF family-based signature predicts prognosis, tumor microenvironment, and molecular subtypes in bladder carcinoma. Front Cell Dev Biol. 2021;9(800967):800967. doi:10.3389/fcell.2021.800967
28. Wilkerson MD, Hayes DN. ConsensusClusterPlus: A class discovery tool with confidence assessments and item tracking. Bioinformatics. 2010;26(12):1572–3. doi:10.1093/bioinformatics/btq170
29. Xu L, Deng C, Pang B, Zhang X, Liu W, Liao G, et al. TIP: A web server for resolving tumor immunophenotype profiling. Cancer Res. 2018;78(23):6575–80. doi:10.1158/0008-5472.CAN-18-0689
30. Chen DS, Mellman I. Oncology meets immunology: The cancer-immunity cycle. Immunity. 2013;39(1):1–10. doi:10.1016/j.immuni.2013.07.012
31. Hu J, Yu A, Othmane B, Qiu D, Li H, Li C, et al. Siglec15 shapes a non-inflamed tumor microenvironment and predicts the molecular subtype in bladder cancer. Theranostics. 2021;11(7):3089–108. doi:10.7150/thno.53649
32. Kamoun A, de Reynies A, Allory Y, Sjodahl G, Robertson AG, Seiler R, et al. A consensus molecular classification of muscle-invasive bladder cancer. Eur Urol. 2020;77(4):420–33. doi:10.1016/j.eururo.2019.09.006
33. Mariathasan S, Turley SJ, Nickles D, Castiglioni A, Yuen K, Wang Y, et al. TGFβ attenuates tumour response to PD-L1 blockade by contributing to exclusion of T cells. Nature. 2018;554(7693):544–8. doi:10.1038/nature25501
34. Sjödahl G, Lauss M, Lövgren K, Chebil G, Gudjonsson S, Veerla S, et al. A molecular taxonomy for urothelial carcinoma. Clin Cancer Res. 2012;18(12):3377–86. doi:10.1158/1078-0432.CCR-12-0077-T
35. Fu H, Zhu Y, Wang Y, Liu Z, Zhang J, Xie H, et al. Identification and validation of stromal immunotype predict survival and benefit from adjuvant chemotherapy in patients with muscle-invasive bladder cancer. Clin Cancer Res. 2018;24(13):3069–78. doi:10.1158/1078-0432.CCR-17-2687
36. McConkey DJ, Choi W. Molecular subtypes of bladder cancer. Curr Oncol Rep. 2018;20(10):77. doi:10.1007/s11912-018-0727-5

37. Robertson AG, Kim J, Al-Ahmadie H, Bellmunt J, Guo G, Cherniack AD, et al. Comprehensive molecular characterization of muscle-invasive bladder cancer. Cell. 2017;171(3):540–56.e25. doi:10.1016/j.cell.2017.09.007
38. Rebouissou S, Bernard-Pierrot I, de Reyniès A, Lepage ML, Krucker C, Chapeaublanc E, et al. EGFR as a potential therapeutic target for a subset of muscle-invasive bladder cancers presenting a basal-like phenotype. Sci Transl Med. 2014;6(244):244ra91. doi:10.1126/scitranslmed.3008970
39. Marzouka NA, Eriksson P, Rovira C, Liedberg F, Sjodahl G, Hoglund M. A validation and extended description of the Lund taxonomy for urothelial carcinoma using the TCGA cohort. Sci Rep. 2018;8(1):3737. doi:10.1038/s41598-018-22126-x
40. Mo Q, Nikolos F, Chen F, Tramel Z, Lee YC, Hayashi K, et al. Prognostic power of a tumor differentiation gene signature for bladder urothelial carcinomas. J Natl Cancer Inst. 2018;110(5):448–59. doi:10.1093/jnci/djx243
41. Damrauer JS, Hoadley KA, Chism DD, Fan C, Tiganelli CJ, Wobker SE, et al. Intrinsic subtypes of high-grade bladder cancer reflect the hallmarks of breast cancer biology. Proc Natl Acad Sci U S A. 2014;111(8):3110–5. doi:10.1073/pnas.1318376111
42. Choi W, Porten S, Kim S, Willis D, Plimack ER, Hoffman-Censits J, et al. Identification of distinct basal and luminal subtypes of muscle-invasive bladder cancer with different sensitivities to frontline chemotherapy. Cancer Cell. 2014;25(2):152–65. doi:10.1016/j.ccr.2014.01.009
43. Seiler R, Ashab HAD, Erho N, van Rhijn BWG, Winters B, Douglas J, et al. Impact of molecular subtypes in muscle-invasive bladder cancer on predicting response and survival after neoadjuvant chemotherapy. Eur Urol. 2017;72(4):544–54. doi:10.1016/j.eururo.2017.03.030
44. Anonymous. Neoadjuvant cisplatin, methotrexate, and vinblastine chemotherapy for muscle-invasive bladder cancer: A randomised controlled trial. International Collaboration of Trialists. Lancet. 1999;354(9178):533–40. doi:10.1016/S0140-6736(99)02292-8
45. Grossman HB, Natale RB, Tangen CM, Speights VO, Vogelzang NJ, Trump DL, et al. Neoadjuvant chemotherapy plus cystectomy compared with cystectomy alone for locally advanced bladder cancer. N Engl J Med. 2003;349(9):859–66. doi:10.1056/NEJMoa022148
46. Fuster MM, Esko JD. The sweet and sour of cancer: glycans as novel therapeutic targets. Nat Rev Cancer. 2005;5(7):526–42. doi:10.1038/nrc1649
47. Ni J, Jiang Z, Shen L, Gao L, Yu M, Xu X, et al. β3GnT8 regulates the metastatic potential of colorectal carcinoma cells by altering the glycosylation of CD147. Oncol Rep. 2014;31(4):1795–801. doi:10.3892/or.2014.3042
48. Liu XS, Liu JM, Chen YJ, Li FY, Wu RM, Tan F, et al. Comprehensive analysis of hexokinase 2 immune infiltrates and m6A related genes in human esophageal carcinoma. Front Cell Dev Biol. 2021;9:715883. doi:10.3389/fcell.2021.715883
49. Liu XS, Liu C, Zeng J, Zeng DB, Chen YJ, Tan F, et al. Nucleophosmin 1 is a prognostic marker of gastrointestinal cancer and is associated with m6A and cuproptosis. Front Pharmacol. 2022;13:1010879. doi:10.3389/fphar.2022.1010879
50. Siegel RL, Miller KD, Fuchs HE, Jemal A. Cancer statistics, 2021. CA Cancer J Clin. 2021;71(1):7–33. doi:10.3322/caac.21654
51. Wu J, Tan Z, Li H, Lin M, Jiang Y, Liang L, et al. Melatonin reduces proliferation and promotes apoptosis of bladder cancer cells by suppressing O-GlcNAcylation of cyclin-dependent-like kinase 5. J Pineal Res. 2021;71(3):e12765. doi:10.1111/jpi.12765
52. Tan Z, Jiang Y, Liang L, Wu J, Cao L, Zhou X, et al. Dysregulation and prometastatic function of glycosyltransferase C1GALT1 modulated by cHP1BP3/miR-1-3p axis in bladder cancer. J Exp Clin Cancer Res. 2022;41(1):228. doi:10.1186/s13046-022-02438-7
53. Beatson R, Tajadura-Ortega V, Achkova D, Picco G, Tsourouktsoglou TD, Klausing S, et al. The mucin MUC1 modulates the tumor immunological microenvironment through engagement of the lectin Siglec-9. Nat Immunol. 2016;17(11):1273–81. doi:10.1038/ni.3552
54. Hu Y, Pan J, Shah P, Ao M, Thomas SN, Liu Y, et al. Integrated proteomic and glycoproteomic characterization of human high-grade serous ovarian carcinoma. Cell Rep. 2020;33(3):108276. doi:10.1016/j.celrep.2020.108276

55. Dyrskjøt L, Ostenfeld MS, Bramsen JB, Silahtaroglu AN, Lamy P, Ramanathan R, et al. Genomic profiling of microRNAs in bladder cancer: miR-129 is associated with poor outcome and promotes cell death in vitro. Cancer Res. 2009;69(11):4851–60. doi:10.1158/0008-5472.CAN-08-4043
56. Fridman WH, Pagès F, Sautès-Fridman C, Galon J. The immune contexture in human tumours: Impact on clinical outcome. Nat Rev Cancer. 2012;12(4):298–306. doi:10.1038/nrc3245
57. Hülsen S, Lippolis E, Ferrazzi F, Otto W, Distel L, Fietkau R, et al. High stroma T-cell infiltration is associated with better survival in stage pT1 bladder cancer. Int J Mol Sci. 2020;21(21):8407. doi:10.3390/ijms21218407
58. Xiao Z, Cai Z, Deng D, Tong S, Zu X. An EMT-based risk score thoroughly predicts the clinical prognosis, tumor immune microenvironment and molecular subtypes of bladder cancer. Front Immunol. 2022;13:1000321. doi:10.3389/fimmu.2022.1000321
59. Cai Z, Chen J, Yu Z, Li H, Liu Z, Deng D, et al. BCAT2 shapes a noninflamed tumor microenvironment and induces resistance to anti-PD-1/PD-L1 immunotherapy by negatively regulating proinflammatory chemokines and anticancer immunity. Adv Sci (Weinh). 2023;10(8):e2207155. doi:10.1002/advs.202207155
60. Li H, Chen J, Li Z, Chen M, Ou Z, Mo M, et al. S100A5 attenuates efficiency of anti-PD-L1/PD-1 immunotherapy by inhibiting CD8+ T cell-mediated anti-cancer immunity in bladder carcinoma. Adv Sci (Weinh). 2023;10(–):e2300110
61. Bajorin DF, Witjes JA, Gschwend JE, Schenker M, Valderrama BP, Tomita Y, et al. Adjuvant nivolumab versus placebo in muscle-invasive urothelial carcinoma. N Engl J Med. 2021;384(22):2102–14. doi:10.1056/NEJMoa2034442
62. Denkert C, von Minckwitz G, Darb-Esfahani S, Lederer B, Heppner BI, Weber KE, et al. Tumour-infiltrating lymphocytes and prognosis in different subtypes of breast cancer: a pooled analysis of 3771 patients treated with neoadjuvant therapy. Lancet Oncol. 2018;19(1):40–50. doi:10.1016/S1470-2045(17)30904-X
63. Goldberg J, Pastorello RG, Vallius T, Davis J, Cui YX, Agudo J, et al. The immunology of hormone receptor positive breast cancer. Front Immunol. 2021;12:674192. doi:10.3389/fimmu.2021.674192
64. Hu J, Othmane B, Yu A, Li H, Cai Z, Chen X, et al. 5mC regulator-mediated molecular subtypes depict the hallmarks of the tumor microenvironment and guide precision medicine in bladder cancer. BMC Med. 2021;19(1):289. doi:10.1186/s12916-021-02163-6
65. Wu X, Ye Y, Vega KJ, Yao J. Consensus molecular subtypes efficiently classify gastric adenocarcinomas and predict the response to anti-PD-1 immunotherapy. Cancers (Basel). 2022;14(15):3740. doi:10.3390/cancers14153740
66. Miao Z, Cao Q, Liao R, Chen X, Li X, Bai L, et al. Elevated transcription and glycosylation of B3GNT5 promotes breast cancer aggressiveness. J Exp Clin Cancer Res. 2022;41(1):169. doi:10.1186/s13046-022-02375-5
67. Hodgson A, Liu SK, Vesprini D, Xu B, Downes MR. Basal-subtype bladder tumours show a “hot” immunophenotype. Histopathology. 2018;73(5):748–57. doi:10.1111/his.13696